

## X-ray photoionization in the presence of a bichromatic laser field

D. B. Milošević

*Department of Physics, Faculty of Science and Mathematics, University of Sarajevo, Zmaja od Bosne 35,  
71000 Sarajevo, Bosnia and Herzegovina  
and Faculty of Mechanical Engineering, University of Sarajevo, 71000 Sarajevo, Bosnia and Herzegovina*

F. Ehlötzky

*Institute for Theoretical Physics, University of Innsbruck, Technikerstrasse 25, A-6020 Innsbruck, Austria  
(Received 6 October 1997; revised manuscript received 21 November 1997)*

X-ray photoionization of hydrogen in the presence of a bichromatic laser field is considered. The expressions for the  $T$  matrix and the cross sections for the laser-assisted x-ray photoionization are presented. The initial state is the laser-field-dressed hydrogen-atom ground state, while the final state is the improved Coulomb-Volkov wave. The gauge consistency is ensured by working in the  $\mathbf{r} \cdot \mathbf{E}$  gauge. It turns out that the matrix elements (the explicit form of which is given in the Appendix) are much simpler in this case. This enables one to consider the symmetry properties of the  $T$  matrix and the cross sections analytically. It was shown that the symmetry  $(\phi + \pi, \pi - \theta) \leftrightarrow (\phi, \theta)$ , where  $\phi$  is the relative phase between the laser-field components and  $\theta$  is the polar angle of the outgoing electron, is exact in our case. In addition to this, there are approximate symmetries  $\phi \leftrightarrow -\phi$  and  $\phi \leftrightarrow \phi + \pi$ . All these symmetries, as well as the behavior of the differential and total cross sections as functions of  $\phi$ ,  $\theta$ , and the number of exchanged photons, are analyzed in numerous examples. The results presented show the possibility of the coherent phase control of the laser-assisted x-ray photoionization process. It was also shown that in the monochromatic case our model gives results that are in good agreement with the results of previous work. [S1050-2947(98)00504-6]

PACS number(s): 32.80.Fb, 32.80.Qk, 32.80.Wr, 32.80.-t

### I. INTRODUCTION

Atomic processes in the presence of strong laser fields are presently attracting considerable attention. Laser-field-induced transitions of an electron from one continuum state to another (free-free transitions) are of special interest because in such processes the absorption or emission of different numbers of photons can occur with comparable probability and the laser-field-matter interaction should be treated nonperturbatively. The observation of the free-free transitions was reported by Weingartshofer *et al.* in experiments on laser-field-assisted electron-atom scattering [1]. Later on such transitions were observed in single- and two-color above-threshold ionization [2,3,28] and in laser-assisted Auger decay [4]. More recently, free-free transitions were studied through the observation of the laser-assisted photoelectric effect [5]. In this experiment soft-x-ray pulses (generated as high-order harmonics of a titanium-sapphire laser) are used for ionization of helium atoms. The modifications of the photoelectron spectra are induced by the fundamental laser-field pulse. In comparison with the photoelectron spectrum in the absence of the laser field one observes the following two modifications: (i) The absorption and emission of laser photons during ionization give rise to sidebands in the spectrum and (ii) the spectrum is shifted to a lower energy as a result of a laser-field-induced increase of the binding energy of the ionized atoms.

Before this observation of the laser-assisted x-ray photoionization such processes were considered theoretically by several authors [6–19]. In these papers the interaction between the atom and the weak high-frequency field (a soft-x-ray field that causes the ionization) is treated perturbatively

to first order. For the soft x rays the dipole approximation is also valid [20]. Concerning the interaction with the strong low-frequency laser field, the approaches of these works are different. Only in the paper by Cionga *et al.* [19] is the dressing of the atomic states by the laser field taken into account. In [6–8,10,14] the outgoing electrons were described by the Volkov waves, while in [9,15–17,19] more adequate Coulomb-Volkov waves were used. In [12,13,18] the low-frequency approximation was considered. It should also be noted that, according to the gauge-invariance requirements, some of the works mentioned are defective (see the first reference in [16]). The papers that consider the two-color above-threshold ionization within the essential states models with the multiple continua should also be mentioned [21]. Recently, two-color processes were analyzed fully nonperturbatively via the numerical solution of the time-dependent Schrödinger equation for a hydrogen atom in the presence of both fields [22].

In this paper we shall consider x-ray photoionization in the presence of a bichromatic low-frequency laser field that consists of two components of frequencies  $\omega$  and  $2\omega$  that are out of phase by an angle  $\phi$ . The study of multiphoton processes in bichromatic laser fields has recently become a subject of particular interest. It was found that by changing the phase  $\phi$  it is possible to increase or decrease the rates of laser-assisted and laser-induced processes. This effect was coined in molecular physics coherent phase control (CPC). In our recent investigation [23,24] a detailed list of references concerning this subject was presented.

In Sec. II we present our theory of photoionization of hydrogen by a high-frequency laser field in the presence of a low-frequency bichromatic laser field. Numerical results for

a monochromatic laser field are presented and compared with the results of other authors in Sec. III, while the results for the bichromatic laser field are presented in Sec. IV. The conclusions are given in Sec. V. In the Appendix we consider the symmetry properties of the  $T$  matrix and the cross sections for the laser-assisted photoionization process. All our results were derived in SI units and the final expressions are presented in the atomic system of units ( $\hbar = e = m = 1$ ).

## II. THEORY

The  $S$ -matrix element for laser-assisted processes with the emission or absorption of one x-ray photon, in the  $\mathbf{r} \cdot \mathbf{E}$  gauge, is

$$S_{fi} = -i \int_{-\infty}^{\infty} dt \langle \Phi_f(t) | \mathbf{r} \cdot \mathbf{E}_X(t) | \Phi_i(t) \rangle = S_{fi}^{(+)} + S_{fi}^{(-)}, \quad (1)$$

where the x-ray electric-field vector is  $\mathbf{E}_X(t) = E_{0X} \hat{\mathbf{e}}_X \sin \omega_X t$ ,  $E_{0X} = I_X^{1/2}$ , and  $\omega_X$ ,  $I_X$ , and  $\hat{\mathbf{e}}_X$  are its frequency, intensity, and unit polarization vector, respectively. The component  $S_{fi}^{(-)} \propto \exp(-i\omega_X t)/2i$  corresponds to the photoionization process we are considering. The initial- and final-state vectors  $|\Phi_j(t)\rangle$ ,  $j = i, f$ , satisfy the Schrödinger equation

$$\left[ i \frac{\partial}{\partial t} - \frac{\mathbf{p}^2}{2} - V - \mathbf{r} \cdot \mathbf{E}(t) \right] |\Phi_j(t)\rangle = 0, \quad j = i, f, \quad (2)$$

where  $V = -1/r$  is the Coulomb potential and the laser-electric-field vector  $\mathbf{E}(t)$ , in our case of a linearly polarized bichromatic laser field (with the same intensity  $I$  of both field components and the unit polarization vector  $\hat{\mathbf{e}}$ ), is given by

$$\mathbf{E}(t) = E_0 \hat{\mathbf{e}} [\sin \omega t + \sin(2\omega t + \phi)], \quad E_0 = I^{1/2}. \quad (3)$$

The initial state  $|\Phi_i(t)\rangle$  is the laser-modified atomic-hydrogen-ground state, which in the first order of time-dependent perturbation theory has the form (see [24–26] and references therein)

$$\begin{aligned} |\Phi_i(t)\rangle &= |\Phi_0(\omega t)\rangle \exp(iI_0 t), \\ |\Phi_0(\varphi)\rangle &= \left\{ 1 - \frac{i}{2} E_0 [G_c(E_0 - \omega) e^{i\varphi} - G_c(E_0 + \omega) e^{-i\varphi}] \right. \\ &\quad \left. + G_c(E_0 - 2\omega) e^{2i\varphi + i\phi} - G_c(E_0 + 2\omega) \right. \\ &\quad \left. \times e^{-2i\varphi - i\phi} \right] \mathbf{r} \cdot \hat{\mathbf{e}} \Big| \psi_0 \rangle. \end{aligned} \quad (4)$$

$G_c(E)$  is the time-independent Coulomb Green's function and  $I_0 = 0.5$  a.u. and  $\psi_0(\mathbf{r}) = \pi^{-1/2} \exp(-r)$  are the ionization energy and the wave function of the ground state of the hydrogen atom, respectively. The final state  $|\Phi_f(t)\rangle$  is the laser-modified atomic-hydrogen continuum state. This state can also be approximated by a perturbative solution, similar to Eq. (4) [24,26], but instead of it we will approximate  $|\Phi_f(t)\rangle$  by the improved Coulomb-Volkov wave [27]

$$\begin{aligned} |\Phi_f(t)\rangle &\approx |\Phi_{\mathbf{k}_f}(t)\rangle \\ &= |\psi_{\mathbf{k}_f + \mathbf{A}(\omega t)}\rangle \exp\{-i[\mathbf{k}_f \cdot \boldsymbol{\alpha}(\omega t) + \mathcal{U}(t) + E_{\mathbf{k}_f} t]\}, \end{aligned} \quad (5)$$

where  $E_{\mathbf{k}_f} = \mathbf{k}_f^2/2$  is the outgoing electron kinetic energy,  $\mathbf{A}(\varphi)$  ( $\varphi = \omega t$ ) is the vector potential of the laser field [ $\mathbf{E}(t) = -\partial \mathbf{A}(\omega t)/\partial t$ ]

$$\mathbf{A}(\varphi) = A_0 \hat{\mathbf{e}} [\cos \varphi + \frac{1}{2} \cos(2\varphi + \phi)], \quad (6)$$

$$\begin{aligned} \boldsymbol{\alpha}(\varphi) &= \int^t dt' \mathbf{A}(\omega t') = \alpha_0 \hat{\mathbf{e}} [\sin \varphi + \frac{1}{4} \sin(2\varphi + \phi)], \\ \alpha_0 &= A_0/\omega = E_0/\omega^2, \end{aligned} \quad (7)$$

$$\mathcal{U}(t) = \frac{1}{2} \int^t dt' \mathbf{A}^2(\omega t') = \frac{5}{4} U_p t + \mathcal{U}_1(\omega t), \quad U_p = A_0^2/4,$$

$$\begin{aligned} \mathcal{U}_1(\varphi) &= \frac{U_p}{\omega} \left[ \frac{1}{2} \sin 2\varphi + \sin(\varphi + \phi) + \frac{1}{3} \sin(3\varphi + \phi) \right. \\ &\quad \left. + \frac{1}{16} \sin(4\varphi + 2\phi) \right], \end{aligned} \quad (8)$$

and  $|\psi_{\mathbf{k}}\rangle$  is the Coulomb wave vector

$$\begin{aligned} \psi_{\mathbf{k}}(\mathbf{r}) &= (2\pi)^{-3/2} \exp[\pi/(2k)] \Gamma(1+i/k) \\ &\quad \times \exp(i\mathbf{k} \cdot \mathbf{r}) {}_1F_1(-i/k, 1 - i(kr + \mathbf{k} \cdot \mathbf{r})). \end{aligned} \quad (9)$$

Introducing Eqs. (4) and (5) into Eq. (1) we obtain

$$S_{fi}^{(-)} = \frac{E_X}{2} \int_{-\infty}^{\infty} dt f(\omega t) \exp[i(E_{\mathbf{k}_f} - \omega_X + I_0 + \frac{5}{4} U_p)t], \quad (10)$$

where

$$f(\varphi) = \langle \psi_{\mathbf{k}_f + \mathbf{A}(\varphi)} | \mathbf{r} \cdot \hat{\mathbf{e}}_X | \Phi_0(\varphi) \rangle \exp\{i[\mathbf{k}_f \cdot \boldsymbol{\alpha}(\varphi) + \mathcal{U}_1(\varphi)]\} \quad (11)$$

is a  $2\pi/\omega$ -periodic function of  $t$  that can be expanded into a Fourier series

$$f(\varphi) = \sum_{n=-\infty}^{\infty} f_n \exp(-in\varphi), \quad f_n = \int_0^{2\pi} \frac{d\varphi}{2\pi} f(\varphi) \exp(in\varphi), \quad (12)$$

so that we obtain

$$S_{fi}^{(-)} = -2\pi i \sum_n \delta(E_{\mathbf{k}_f} + I_0 + \frac{5}{4} U_p - \omega_X - n\omega) T_{fi}(n), \quad (13)$$

where  $T_{fi}(n) = (i/2) E_X f_n$  is the  $T$ -matrix element for the exchange of  $n$  laser photons (in addition to the absorption of one x-ray photon). The processes with  $n < 0$  correspond to stimulated emission, while the processes with  $n > 0$  correspond to the absorption of  $n$  photons. The matrix elements that appear in  $f(\varphi)$  can be computed analytically (see the Appendix). For the computation of the matrix elements with the time-independent Coulomb Green's functions its Sturmian representation can be used, but, in our case, as it was shown in [25], the closure approximation with the mean en-

ergy  $\bar{E}_0=4/9$  a.u. gives satisfactory results. Therefore, we are left with one numerical integration over  $\varphi$  that can be easily done. From the energy-conserving condition  $E_{\mathbf{k}_f} = \omega_X + n\omega - I_0 - \frac{5}{4}U_p$  it follows that the laser field induces an increase of the binding energy by  $\frac{5}{4}U_p$  that is in agreement with the experiment [5] (for a monochromatic laser field this increase is  $U_p$ , while for our bichromatic field we have an extra increase by  $U_p/4$  because of the  $2\omega$  field component).

The differential cross section (DCS) that corresponds to the exchange of  $n$  laser photons, normalized to the flux of incident x-ray photons, is defined by [20]

$$\frac{d\sigma(n)}{d\Omega} = 2\pi \frac{\omega_X}{I_X} k_f(n) |T_{fi}(n)|^2, \quad (14)$$

where  $k_f(n) = (2E_{\mathbf{k}_f})^{1/2}$  is determined by the energy-conserving condition. The total cross section (TCS) for the exchange of  $n$  photons is

$$\sigma(n) = \int d\Omega \frac{d\sigma(n)}{d\Omega}. \quad (15)$$

Denoting by  $n_0$  the smallest negative integer for which  $\mathbf{k}_f^2$  is still positive, one obtains for the TCS (summed over all  $n$ )

$$\sigma_{\text{tot}} = \sum_{n=n_0}^{\infty} \sigma(n). \quad (16)$$

### III. NUMERICAL RESULTS: MONOCHROMATIC LASER FIELD

We shall first compare our results for the x-ray photoionization cross sections in the presence of a monochromatic laser field with the results of Refs. [15,22,19]. In the paper by Leone *et al.* [15] the initial state was the ground state of the hydrogen atom and the final state was the Coulomb-Volkov wave with an extra gauge factor  $|\Phi_f(t)\rangle = \exp[i\mathbf{A}(\omega t) \cdot \mathbf{r}] |\psi_{\mathbf{k}_f}\rangle \exp\{-i[\mathbf{k}_f \cdot \boldsymbol{\alpha}(\omega t) + \mathcal{U}(t) + E_{\mathbf{k}_f} t]\}$ . The agreement between their and our results is good for low laser-field intensities. For the higher intensities we have noticed some differences. As an example of this, in Fig. 1 we present the TCS as a function of the number  $n$  of exchanged photons for  $\omega=1.17$  eV,  $\omega_X=50$  eV, and  $I=5 \times 10^{12}$  W/cm<sup>2</sup>. These results correspond to the results presented in Fig. 5 in [15]. Filled circles on our figure correspond to the  $\sigma(n)$  defined without the factor  $k_f$  (as it was done in [15]; this factor comes from the density of the final state). One can notice that for  $|n| < 8$  the sidebands that correspond to the stimulated emission processes are larger than those of the absorption. This is more pronounced than in [15]. For higher intensities and frequencies these differences become more important and they are significant close to the threshold  $n = n_0$ . In order to illustrate this, in Fig. 2 we present the TCS  $\sigma(n)$  as a function of the photoelectron energy for  $\omega=1.55$  eV,  $\omega_X=13\omega$ , and (a)  $I=5 \times 10^{11}$  W/cm<sup>2</sup>, (b)  $I=3 \times 10^{12}$  W/cm<sup>2</sup>, and (c)  $I=1.75 \times 10^{13}$  W/cm<sup>2</sup>. These results correspond to the results of Fig. 2 in the paper by Vénier *et al.* [22]. In [22] the photoelectron spectra are obtained via the numerical solution of the time-dependent Schrödinger equa-

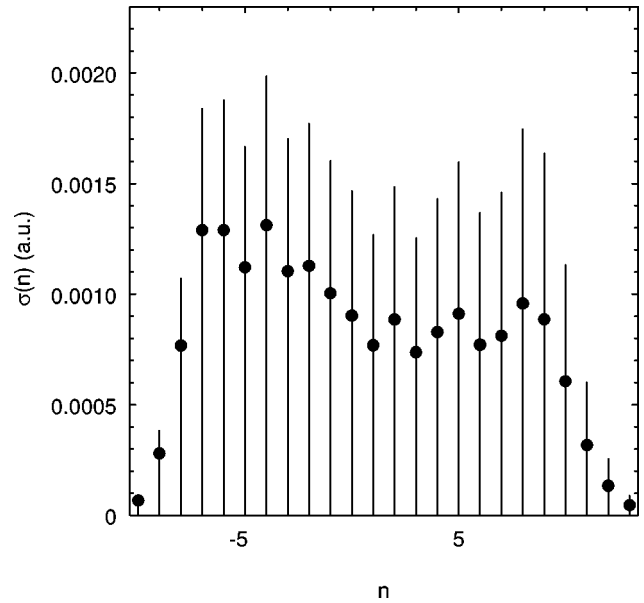


FIG. 1. The TCS (in a.u.) for the photoionization process in the presence of a monochromatic laser field as a function of the number  $n$  of exchanged photons for  $\omega=1.17$  eV,  $\omega_X=50$  eV, and  $I=5 \times 10^{12}$  W/cm<sup>2</sup>. Filled circles correspond to the  $\sigma(n)$  defined without the factor  $k_f$ .

tion for a hydrogen atom in the presence of both fields. The authors claim that they verified that their results are quite different from the results of Leone *et al.* [15]. This means that the approach of Leone *et al.* is not applicable for the laser field parameters considered in [22]. However, as our Fig. 2 shows, our method gives quite satisfactory results. The only difference between the results of Vénier *et al.* [22] and our results appears for Fig. 2(c), where our peaks are slightly suppressed close to the threshold. This difference is expected because for small values of  $E_{\mathbf{k}_f}$  the influence of the atomic hydrogen bound states (which is not taken into account in our improved Coulomb-Volkov waves) becomes important. All other features of the photoelectron spectra presented in [22] are recovered.

We have also compared our results with the results of work by Cionga *et al.* [19]. They have presented the DCS as a function of the polar angle  $\theta$  for two different geometries:  $\hat{\mathbf{e}} \parallel \hat{\mathbf{e}}_X$  (in this case the results do not depend on the azimuthal angle; the results of our Figs. 1 and 2 are for the parallel geometry case) and  $\hat{\mathbf{e}} \perp \hat{\mathbf{e}}_X$  (with the azimuthal angle equal to  $\pi/2$ ). Unfortunately, in [19] the influence of the ponderomotive potential was neglected. They considered two cases of the high-frequency photon energy:  $\omega_X=16$  eV and  $\omega_X=50$  eV, and the cases  $n=\pm 1$ . The chosen laser-electric-field strengths were  $E_0=0.01, 0.02,$  and  $0.03$  a.u., which (for  $\omega=1.17$  eV) correspond to  $U_p=0.368, 1.47,$  and  $3.31$  eV, respectively. Our energy-conserving condition, for  $\omega_X=16$  eV, gives  $E_{\mathbf{k}_f} = (2.39 \pm 1.17)$  eV  $- U_p$ , which shows that, in this case, the neglect of  $U_p$  is a very crude approximation. In the case of  $n=-1$  and  $E_0=0.03$  a.u., one even obtains  $E_{\mathbf{k}_f} < 0$ , which is impossible. Therefore, we will consider only the case  $\omega_X=50$  eV, for which  $U_p$  can be neglected. We found good agreement. This can be seen by comparing our results presented in Fig. 3 and the results of their Figs. 4(b),

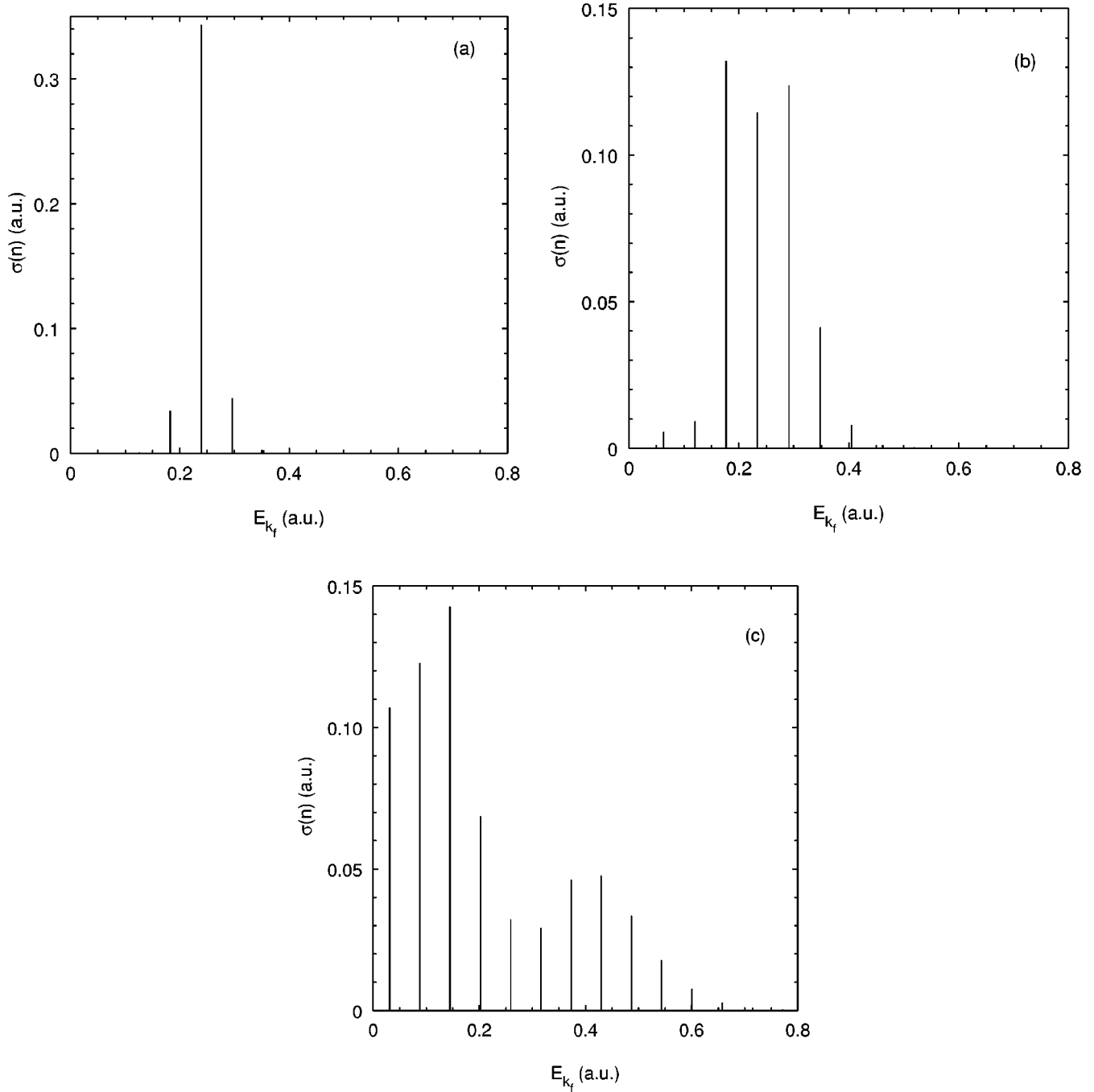


FIG. 2. The TCS as a function of the photoelectron energy for the monochromatic laser field of frequency  $\omega = 1.55$  eV,  $\omega_X = 13\omega$ , and (a)  $I = 5 \times 10^{11}$  W/cm<sup>2</sup>, (b)  $I = 3 \times 10^{12}$  W/cm<sup>2</sup>, and (c)  $I = 1.75 \times 10^{13}$  W/cm<sup>2</sup>.

6(b), and 8(b). We have also taken into account that their definition of the DCS is different from ours by the factor  $2/k_f$ .

#### IV. NUMERICAL RESULTS: BICHROMATIC LASER FIELD

In the case of a bichromatic laser field we have an additional parameter: the relative phase  $\phi$  between the laser-field components. The exact and the approximate symmetry properties of the  $T$  matrix and the cross sections are analyzed in the Appendix. In order to illustrate these symmetries, in Fig.

4 we present the results for the DCS for one-photon absorption, parallel geometry, and  $\omega = 1.17$  eV,  $\omega_X = 50$  eV, and  $I = 3.51 \times 10^{12}$  W/cm<sup>2</sup>. From Fig. 4 the approximate symmetry  $\phi \leftrightarrow 2\pi - \phi$  and the exact symmetry  $(\phi, \theta) \leftrightarrow (\phi + \pi, \pi - \theta)$  can be easily recognized.

Let us now consider the TCS for the same values of the frequencies  $\omega$  and  $\omega_X$  and the intensity  $I$  as in Fig. 1. Our numerical results show that the TCS changes significantly with the change of the phase  $\phi$  and that the TCS exhibits the exact  $\sigma(n, \phi + \pi) = \sigma(n, \phi)$  symmetry and the approximate symmetry  $\sigma(n, 2\pi - \phi) \approx \sigma(n, \phi)$ , which is discussed in the Appendix. In Fig. 5 we compare the monochromatic results

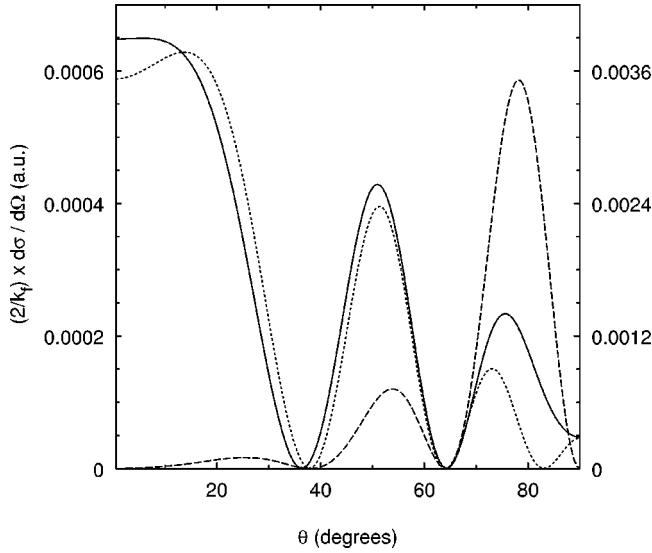


FIG. 3. The DCS, multiplied by the factor  $2/k_f$ , as a function of the scattering angle  $\theta$  for the monochromatic laser-electric-field strength  $E_0=0.01$  a.u.,  $\omega=1.17$  eV, and  $\omega_X=50$  eV. Continuous and dotted curves corresponds to the parallel geometry ( $\hat{\mathbf{e}}\parallel\hat{\mathbf{e}}_X$ ) and to the left ordinate's scale, while the dashed curve correspond to the perpendicular geometry ( $\hat{\mathbf{e}}\perp\hat{\mathbf{e}}_X$ ) with the azimuthal angle equal to  $\pi/2$  and to the right scale. The continuous curve corresponds to the stimulated emission of one laser field photon, while the dotted and dashed curves correspond to the absorption of one photon.

(continuous bars) of Fig. 1 with the bichromatic results with  $\phi=0$  (dotted line with the filled circles) and  $\phi=\pi/2$  (dashed line with the triangles). Contrary to the monochromatic case, the  $\phi=\pi/2$  curve has a pronounced maximum for  $n=0$ , while the  $\phi=0$  curve has two maxima around  $n=\pm 5$ , with a minimum between them. This behavior of the TCS can be connected with the behavior of the generalized Bessel functions.

Finally, in Fig. 6 we present a series of results for the DCS as a function of  $\phi$  and  $\theta$  for the different values of  $n$  and for the laser and x-ray field parameters as in Fig. 3. The geometry is parallel. The conclusion is that we have a strong CPC effect that also depends on the number of exchanged photons.

## V. CONCLUSIONS

We have presented analytical and numerical results for the x-ray photoionization of hydrogen in the presence of a bichromatic linearly polarized laser field. Choosing for the final outgoing electron state the improved Coulomb-Volkov wave (which in the  $\mathbf{r}\cdot\mathbf{E}$  gauge has a simple form without the Goepfert-Mayer factor) and for the initial state the laser-field-dressed hydrogen-atom ground state, we ensured both the gauge consistency of the problem and the simple form of the matrix elements. The contributions of the laser-field dressing of the ground state are small and can be treated within the closure approximation. Using these results we were able to show that the cross sections are invariant under the substitution  $(\phi+\pi, \pi-\theta)\leftrightarrow(\phi, \theta)$  and that there are also approximate symmetries  $\phi\leftrightarrow-\phi$  and  $\phi\leftrightarrow\phi+\pi$ . Our numerical results confirm these symmetries. They also show a significant CPC effect that depends on the number of ex-

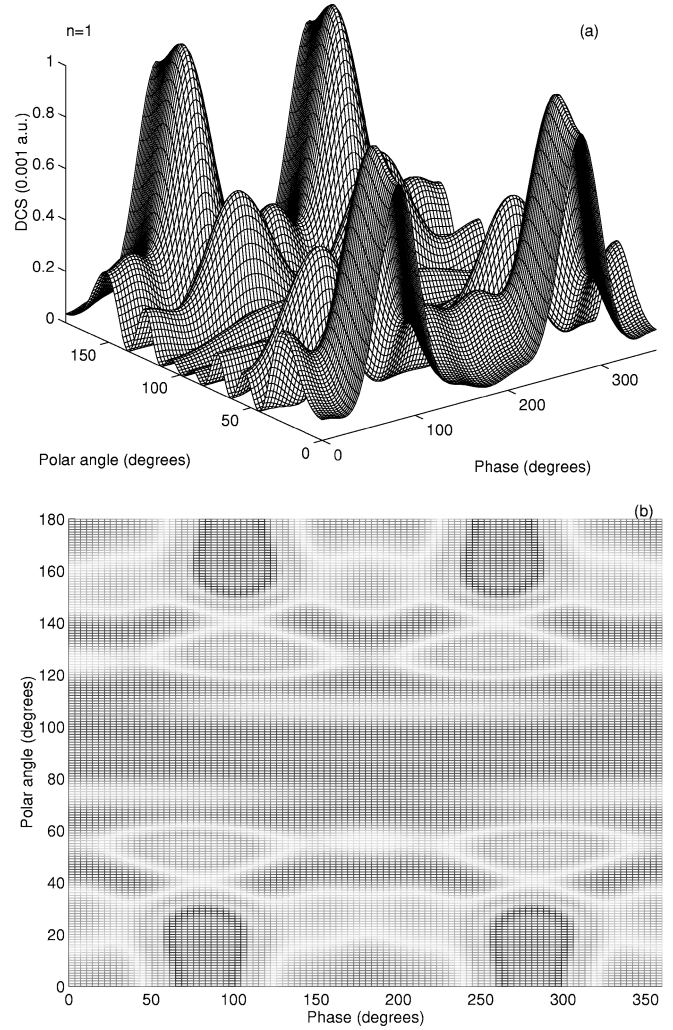


FIG. 4. The DCS for the x-ray ( $\omega_X=50$  eV) photoionization assisted by a bichromatic laser field of frequency  $\omega=1.17$  eV and intensity  $I=3.51\times 10^{12}$  W/cm<sup>2</sup> as a function of the relative phase  $\phi$  and the polar angle  $\theta$ , for one absorbed photon. The geometry is parallel.

changed photons and on the geometry of the photoionization process.

## ACKNOWLEDGMENTS

D. M. thanks the Institute for Theoretical Physics, University of Innsbruck for its hospitality and financial support. This work has been supported by the Jubilee Foundation of the Austrian National Bank under Project No. 6211/1 and by the East-West Program of the Austrian Academy of Sciences and the Austrian Ministry of Science and Transportation under Project No. 45.372/2-IV/6/97.

## APPENDIX

In this appendix we shall consider the symmetry properties of the  $T$  matrix and the cross sections for the laser-assisted photoionization process. The outgoing electron momentum in the spherical coordinates is  $\mathbf{k}_f=k_f(\sin\theta\cos\varphi\hat{\mathbf{x}}+\sin\theta\sin\varphi\hat{\mathbf{y}}+\cos\theta\hat{\mathbf{z}})$ . We choose the laser-field polarization

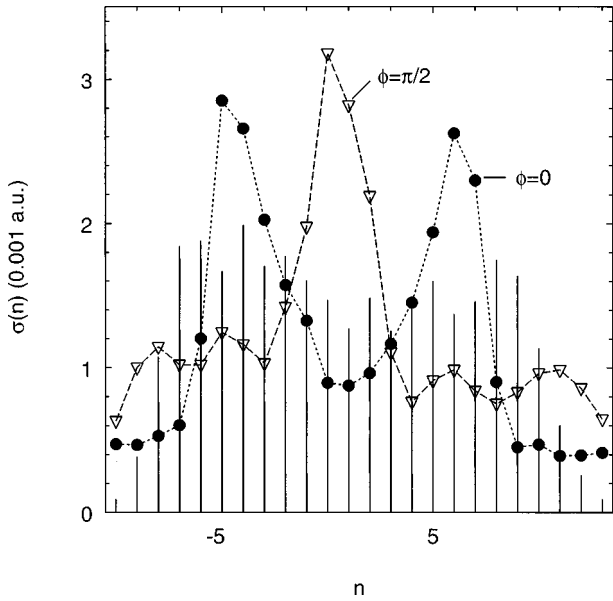


FIG. 5. The TCS as a function of the number of exchanged photons  $n$  for the same parameters as in Fig. 1 and the parallel geometry. Continuous bars correspond to the monochromatic case, while the dotted curve with the filled circles and the dashed curve with the triangles correspond to the phase  $\phi=0$  and  $\phi=\pi/2$ , respectively.

vector along the  $z$  axis, so that  $\hat{\mathbf{e}} \cdot \mathbf{k}_f = k_f \cos \theta$ . For the  $x$  ray polarization vector we consider (as in [19]) two configurations: parallel geometry with  $\hat{\mathbf{e}}_X \parallel \hat{\mathbf{e}}$  and perpendicular geometry with  $\hat{\mathbf{e}}_X \perp \hat{\mathbf{e}}$ . For the parallel geometry the results do not

depend on  $\varphi_f$  and the integral over  $\varphi_f$  in the TCS gives a factor  $2\pi$ . For the perpendicular geometry we choose  $\hat{\mathbf{e}}_X = \hat{\mathbf{y}}$  and  $\varphi_f = \pi/2$ , so that  $\hat{\mathbf{e}}_X \cdot \mathbf{k}_f = k_f \sin \theta$ . According to the results of Sec. II, the  $T$  matrix can be written in the form

$$T_{fi}(n; \phi, \theta) = \int_0^{2\pi} d\varphi M(\varphi; \phi, \theta) \exp[i g(n; \varphi, \phi, \theta)], \quad (\text{A1})$$

where

$$M(\varphi; \phi, \theta) = \frac{i}{4\pi} E_X \sum_{m=0, \pm 1, \pm 2} M_m(\varphi; \phi, \theta), \quad (\text{A2})$$

with

$$M_0(\varphi; \phi, \theta) = \langle \psi_{\mathbf{k}(\varphi)} | \mathbf{r} \cdot \hat{\mathbf{e}}_X | \psi_0 \rangle, \quad \mathbf{k}(\varphi) = \mathbf{k}_f + \mathbf{A}(\varphi), \quad (\text{A3})$$

and (in the closure approximation)

$$M_m(\varphi; \phi, \theta) = \frac{\pm i E_0}{2(\bar{E}_0 + m\omega)} \langle \psi_{\mathbf{k}(\varphi)} | \mathbf{r} \cdot \hat{\mathbf{e}}_X \mathbf{r} \cdot \hat{\mathbf{e}} | \psi_0 \rangle \times \exp[im\varphi \pm i\delta_{|m|,2}\phi], \quad (\text{A4})$$

where  $m = \pm 1, \pm 2$ ,  $\bar{E}_0 = 4/9$  a.u., and the plus (minus) sign stands for  $m > 0$  ( $m < 0$ ). The function  $g(n; \varphi, \phi, \theta)$ , in the exponent of Eq. (A1), is defined as

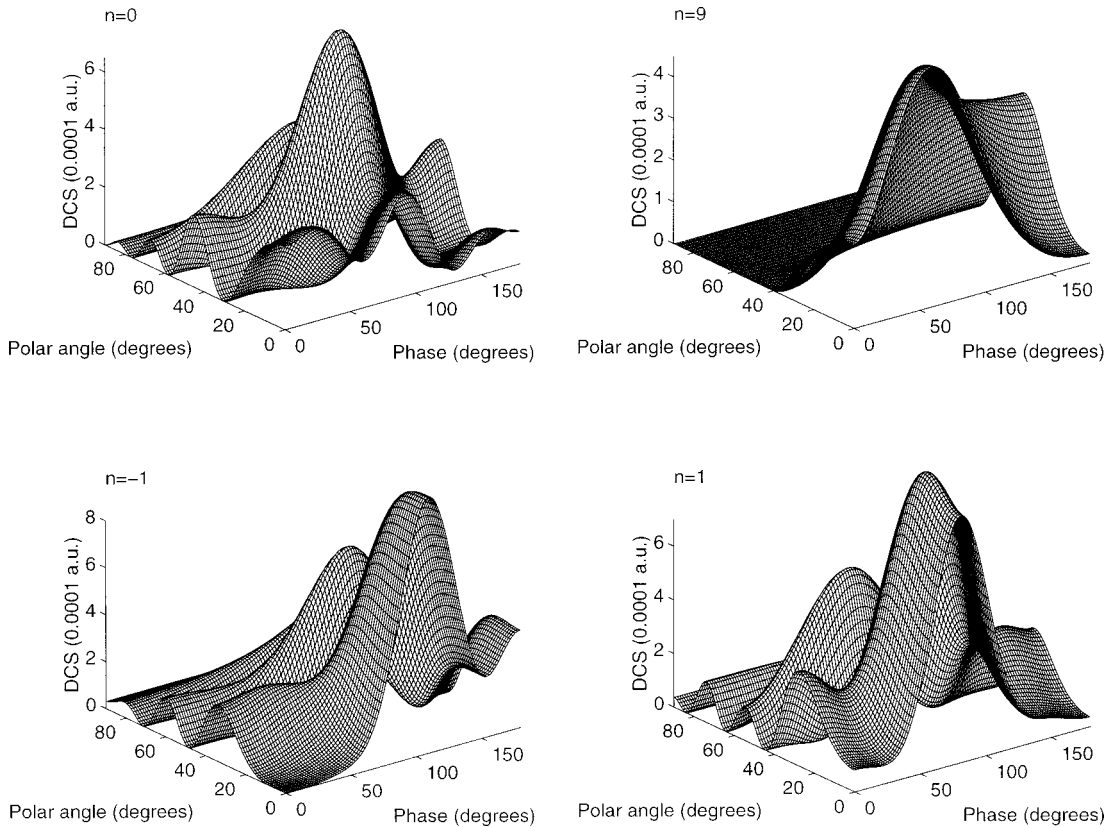


FIG. 6. The DCS as a function of the phase  $\phi$  and the polar angle  $\theta$  for different numbers of exchanged photons ( $n=0, 9, -1, 1$ ) and the parallel geometry. The other parameters are as in Fig. 3.

$$g(n; \varphi, \phi, \theta) = k_f \alpha_0 \cos \theta [\sin \varphi + \frac{1}{4} \sin(2\varphi + \phi)] + \mathcal{U}_1(\varphi, \phi) + n\varphi, \quad (\text{A5})$$

where  $\mathcal{U}_1(\varphi, \phi)$  is given by Eq. (8). Using Eqs. (4) and (9), for the explicit form of the matrix elements that appear in  $M_m$ , we obtain

$$\langle \psi_{\mathbf{k}} | \mathbf{r} \cdot \hat{\mathbf{e}}_X | \psi_0 \rangle = -i \frac{2^{5/2}}{\pi} \frac{\hat{\mathbf{e}}_X \cdot \hat{\mathbf{k}}}{(1+k^2)^2(k+i)} \left( \frac{i-k}{i+k} \right)^{i/k} \times \Gamma(1-i/k) \exp[\pi/2k] \quad (\text{A6})$$

and

$$\begin{aligned} \langle \psi_{\mathbf{k}} | \mathbf{r} \cdot \hat{\mathbf{e}}_X \mathbf{r} \cdot \hat{\mathbf{e}} | \psi_0 \rangle &= -\frac{2^{7/2}}{\pi} \left\{ \frac{\hat{\mathbf{e}} \cdot \hat{\mathbf{k}} \hat{\mathbf{e}}_X \cdot \hat{\mathbf{k}}}{(1+k^2)^4(k+i)} [(k-2i)(1+k^2)+3k] \right. \\ &\quad \left. - \frac{\hat{\mathbf{e}}_X \cdot \hat{\mathbf{e}}}{(1+k^2)^2(k+i)^2} \right\} \left( \frac{i-k}{i+k} \right)^{i/k} \Gamma(1-i/k) \exp[\pi/2k]. \end{aligned} \quad (\text{A7})$$

Using these results we found the symmetry property

$$T_{fi}(n; \phi + \pi, \pi - \theta) = \mp (-1)^n T_{fi}(n; \phi, \theta), \quad (\text{A8})$$

where the minus and plus signs stand for parallel and perpendicular geometries, respectively. Therefore, if the results for the DCS are known for  $0 \leq \theta \leq \pi/2$ ,  $0 \leq \phi \leq 2\pi$ , then the results for  $\pi/2 < \theta \leq \pi$  can be obtained using Eq. (A8). The results of this type follow from general considerations about the relation between a shift in relative phase by  $\pi$  and a shift in the origin of time and space inversion (see, for example, [2]).

In addition to the symmetry (A8) there are also some approximate symmetries. We should take into account that for the higher laser-field intensities multiphoton ionization processes become important. Because we are not considering such processes, there is an upper limit on the laser-field intensity for which our theory can be applied. For the laser frequency  $\omega = 1.17$  eV the critical intensity is of order  $10^{13}$  W/cm<sup>2</sup>. In this case our numerical results show that the corrections due to the dressing of the ground state are small and one can neglect the contribution of the matrix elements  $M_m$ ,  $m = \pm 1, \pm 2$ , which are proportional to  $E_0 = I^{1/2}$  [Eq. (A4)]. In this case, after the substitution  $(\varphi, \phi) \rightarrow (-\varphi, -\phi)$  in Eq. (A1), one obtains the approximate relation for the  $T$  matrix

$$T_{fi}^*(n; -\phi, \theta) = \int_0^{2\pi} d\varphi M^*(\varphi; \phi, \theta) \exp[ig(n; \varphi, \phi, \theta)]. \quad (\text{A9})$$

If  $|\arg M(\varphi; \phi, \theta)| \ll |g(n; \varphi, \phi, \theta)|$ , then the DCS satisfies the relation

$$\frac{d\sigma(n; -\phi, \theta)}{d\Omega} \approx \frac{d\sigma(n; \phi, \theta)}{d\Omega}. \quad (\text{A10})$$

The same symmetry is satisfied in the opposite case when  $|\arg M(\varphi; \phi, \theta)| \gg |g(n; \varphi, \phi, \theta)|$  [in this case one should compare  $T_{fi}(n; -\phi, \theta)$ , instead of  $T_{fi}^*(n; -\phi, \theta)$ , with  $T_{fi}(n; \phi, \theta)$ ]. Of course, because  $g(n; \varphi, \phi, \theta)$  depends on  $\cos \theta$ , there is a small interval of  $\theta$  for which the relation (A10) is not satisfied.

In addition to the symmetries (A8) and (A10) there is also an approximate symmetry

$$\frac{d\sigma(n; \phi + \pi, \theta)}{d\Omega} \approx \frac{d\sigma(n; \phi, \theta)}{d\Omega}, \quad (\text{A11})$$

which is connected with the following property of the generalized Bessel functions (see, for example, [29]):

$$\begin{aligned} B_n(a, b; \phi) &= \int_0^{2\pi} \frac{d\varphi}{2\pi} \exp\{i[a \sin \varphi + b \sin(2\varphi + \phi) - n\varphi]\} \\ &= (-1)^n B_n^*(a, b; \phi + \pi). \end{aligned} \quad (\text{A12})$$

Namely, if the contribution of  $\mathcal{U}_1(\varphi, \phi)$  in Eq. (A5) is small, then the function  $g(n; \varphi, \phi, \theta)$  is of the same form as the exponent of the function under the integral that defines the generalized Bessel function. For example, for  $\omega = 1.17$  eV,  $\omega_X = 50$  eV, and  $I = 5 \times 10^{12}$  W/cm<sup>2</sup>, which corresponds to the parameters of our Fig. 5, it is  $\mathcal{U}_1(\varphi, \phi) \sim U_p/2\omega = 0.224$  a.u.  $\ll k_f \alpha_0 \sim 10$  a.u., so that  $\mathcal{U}_1(\varphi, \phi)$  can be neglected. If the matrix elements that appear in  $M(\varphi; \phi, \theta)$  are slowly varying functions of  $\varphi$ , they can be extracted out of the integral over  $\varphi$  and we will just rest with the generalized Bessel function  $B_{-n}(a, a/4; \phi)$ ,  $a = k_f \alpha_0 \cos \theta$ , which explains the symmetry property (A11). From Eq. (A8) it follows that the TCS (for parallel geometry) satisfies the symmetry property  $\sigma(n, \phi + \pi) = \sigma(n, \phi)$  and the approximate symmetry  $\sigma(n, -\phi) \approx \sigma(n, \phi)$ .

- [1] A. Weingartshofer, J. K. Holmes, G. Caudle, and H. Krüger, Phys. Rev. Lett. **39**, 269 (1977).  
 [2] H. G. Muller, H. B. van Linden van den Heuvell, and M. J. van der Wiel, J. Phys. B **19**, L733 (1986).  
 [3] R. R. Freeman and P. H. Bucksbaum, J. Phys. B **24**, 325 (1991).  
 [4] J. M. Schins, P. Breger, P. Agostini, R. C. Constantinescu, H.

- G. Muller, G. Grillon, A. Antonetti, and A. Mysyrowicz, Phys. Rev. Lett. **73**, 2180 (1994).  
 [5] T. E. Glover, R. W. Schoenlein, A. H. Chin, and C. V. Shank, Phys. Rev. Lett. **76**, 2468 (1996).  
 [6] I. Freund, Opt. Commun. **8**, 401 (1973).  
 [7] F. Ehlötzky, Opt. Commun. **13**, 1 (1975); **25**, 221 (1978); **40**,

- 135 (1981); Phys. Lett. **69A**, 24 (1978); J. Phys. B **20**, 2619 (1987); **22**, 601 (1989).
- [8] N. Tzoar and M. Jain, Opt. Commun. **19**, 417 (1976); **24**, 153 (1978); M. Jain and N. Tzoar, Phys. Rev. A **15**, 147 (1977).
- [9] G. Ferrante, E. Fiordilino, and L. Lo Cascio, Phys. Lett. **81A**, 261 (1981).
- [10] G. Ferrante, E. Fiordilino, and M. Rapisarda, J. Phys. B **14**, L497 (1981).
- [11] L. C. M. Miranda, Phys. Lett. **86A**, 363 (1981); G. Ferrante, E. Fiordilino, and C. Leone, *ibid.* **92A**, 276 (1982).
- [12] E. Fiordilino and M. H. Mittleman, Phys. Rev. A **28**, 229 (1983).
- [13] M. Dörr and R. Shakeshaft, Phys. Rev. A **36**, 421 (1987).
- [14] A. L. A. Fonseca and O. A. C. Nunes, Phys. Rev. A **37**, 400 (1988).
- [15] C. Leone, S. Bivona, R. Burlon, and G. Ferrante, Phys. Rev. A **38**, 5642 (1988).
- [16] P. Kálmán, Phys. Rev. A **39**, 2428 (1989); **38**, 5458 (1988); **39**, 3200 (1989).
- [17] S. Bivona, R. Burlon, C. Leone, and G. Ferrante, Nuovo Cimento D **11**, 1751 (1989).
- [18] F. Ehlotzky, Can. J. Phys. **70**, 731 (1992).
- [19] A. Cionga, V. Florescu, A. Maquet, and R. Taïeb, Phys. Rev. A **47**, 1830 (1993).
- [20] C. J. Joachain *Quantum Collision Theory* (North-Holland/American Elsevier, Amsterdam, 1975).
- [21] K. Rzzewski, L. Wang, and J. W. Haus, Phys. Rev. A **40**, 3453 (1989); L. Wang, J. W. Haus, and K. Rzzewski, *ibid.* **42**, 6784 (1990); R. Buffa, S. Cavalieri, R. Eramo, and M. Matera, J. Opt. Soc. Am. B **13**, 492 (1996).
- [22] V. Vénard, R. Taïeb, and A. Maquet, Phys. Rev. Lett. **74**, 4161 (1995).
- [23] S. Varró and F. Ehlotzky, J. Phys. B **30**, 1061 (1997).
- [24] D. B. Milošević and F. Ehlotzky, Phys. Rev. A **56**, 3879 (1997).
- [25] D. B. Milošević F. Ehlotzky, and B. Piraux, J. Phys. B **30**, 4347 (1997).
- [26] P. Martin, V. Vénard, A. Maquet, P. Francken, and C. J. Joachain, Phys. Rev. A **39**, 6178 (1989).
- [27] J. Z. Kamiński, Phys. Scr. **34**, 770 (1986); P. S. Krstić and D.B. Milošević, J. Phys. B **20**, 3487 (1987); R. Shakeshaft and R. M. Potvliege, Phys. Rev. A **36**, 5478 (1987); M. H. Mittleman, *ibid.* **50**, 3249 (1994); J. Z. Kamiński, A. Jaroń, and F. Ehlotzky, *ibid.* **53**, 1756 (1996).
- [28] H. G. Muller, P. H. Bucksbaum, D. W. Schumacher, and A. Zavriyev, J. Phys. B **23**, 2761 (1990); R. M. Potvliege and P. H. G. Smith, *ibid.* **25**, 2501 (1992).
- [29] S. Varró and F. Ehlotzky, J. Phys. B **28**, 1613 (1995).